Miner Deposita (2007) 42:293–299
DOI 10.1007/s00126-006-0109-z

LETTER

CO_2-rich fluid inclusions with chalcopyrite daughter mineral from the Fenghuangshan Cu–Fe–Au deposit, China: implications for metal transport in vapor

Jianqing Lai · Guoxiang Chi

Received: 8 June 2006 / Accepted: 18 October 2006 / Published online: 4 January 2007

Abstract CO_2-rich fluid inclusions containing opaque mineral crystals were found in the Fenghuangshan skarn-porphyry Cu–Fe–Au deposit in Tongling, Anhui, China. These inclusions show variable CO_2 contents and are accompanied by aqueous inclusions, both occurring as secondary inclusions in quartz and being locally associated with chalcopyrite mineralization. Laser Raman microspectroscopic analyses confirm the predominance of CO_2 in the vapor and the presence of H_2S as high as 8 mol%, and identify the opaque mineral with yellow reflectance color in the inclusions as chalcopyrite. More than half of the CO_2-bearing inclusions contains chalcopyrite, whereas few of the associated aqueous inclusions do so. The chalcopyrite, occupying less than 1% (volume) of the inclusions, is interpreted to be a daughter mineral, and calculated Cu concentrations in the inclusions range from 0.1 to 3.4 wt%. Copper is inferred to have been transported in CO_2-dominated fluids as HS^- complexes. The occurrence of chalcopyrite daughter crystals in CO_2-rich fluid inclusions indicates that CO_2-rich vapor has the capacity of transporting large amounts of Cu, and possibly Au. This finding has significant implications for metal transport and mineralization in hydrothermal systems enriched in CO_2, such as orogenic-type and granitic intrusion-related gold deposits.

Editorial handling: L. Meinert

J. Lai
School of Geoscience and Environmental Engineering,
Central South University,
Changsha, Hunan 410083, China

J. Lai · G. Chi (✉)
Department of Geology, University of Regina,
Regina, Saskatchewan S4S 0A2, Canada
e-mail: guoxiang.chi@uregina.ca

Keywords CO_2-rich inclusions · Daughter mineral · Metal transport · Vapour

Introduction

In hydrothermal mineralizing systems metals are generally considered to be transported as complexes in aqueous liquid (e.g., Barnes 1979). However, as summarized by Williams-Jones and Heinrich (2005), more and more evidence indicates that vapor can also transport large amounts of metals, and some metals (notably Cu and Au) are even preferentially transported by vapor rather than liquid in some magmatic hydrothermal systems (Heinrich et al. 1999). The most direct evidence of high concentrations of metal in vapor is the presence of metallic daughter minerals in vapor inclusions; so far such inclusions were reported mainly in porphyry copper deposits, with the vapor being dominated by water (Williams-Jones and Heinrich 2005 and references therein). Other studies of metal transport in vapor, including analysis of volcanic gases and their sublimates and experimental studies of metal solubility (see Williams-Jones and Heinrich 2005), also mainly deal with fluid systems dominated by water. On the other hand, a few recent studies have indicated that metals can be transported in nonaqueous vapor, with CO_2 (Yang and Scott 1996; Schmidt Mumm et al. 1997; Chi et al. 2005, 2006) or CH_4 (Hanley et al. 2005) as dominant components. In this paper, we report CO_2-rich fluid inclusions that contain chalcopyrite daughter crystals from a skarn-porphyry Cu–Fe–Au deposit (Fenghuangshan, Tongling, China), providing direct support of the potential of water-poor vapor to carry high concentrations of copper. Although these inclusions only occur locally and do not represent the fluids that were mainly responsible for the formation of the

Fenghuangshan deposit, where the dominant fluid inclusions belong to aqueous salt types (Lai et al., in preparation), their implications for metal transport in nonaqueous vapor cannot be neglected.

Geologic background and study methods

The Fenghuangshan Cu–Fe–Au deposit, located in Tongling, Anhui Province, China, is one of the more than 200 Cu, Fe, Au, Mo, Zn, Pb, Ag deposits related to Yanshanian (Jurassic to Cretaceous) intermediate to felsic intrusions in the Middle-Lower Yangtze River polymetallic belt (Chang et al. 1991; Pan and Dong 1999). The deposit was first formed as a skarn-type deposit in the contact zone between a Late Yanshanian granodiorite intrusion and Lower Triassic limestones, and then overprinted by porphyry-type mineralization related to quartz monzodiorite porphyry stocks. The skarn-type mineralization is characterized by chalcopyrite and bornite cutting and replacing magnetite that postdates an assemblage of massive garnet with some diopside and wollastonite. The porphyry-type mineralization occurs in quartz monzodiorite porphyry bodies that crosscut the skarn, and consists of four successive mineralization stages characterized by quartzification (stage I), garnet infill and recrystallization (II), quartz, chalcopyrite, and bornite veinlets dissemination (III), and calcite veinlets (IV). Stage I quartz and stage II garnet are characterized by development of halite-bearing aqueous inclusions, whereas stage III quartz and stage IV calcite contain aqueous inclusions without salt daughter minerals (Lai et al., in preparation). CO_2-rich fluid inclusions and associated aqueous inclusions of secondary origin were found locally in stage I quartz, and are spatially associated with chalcopyrite, which occurs along microfractures or in irregular patches in quartz (Fig. 1a).

The petrography of fluid inclusions (modes of occurrence and phase assemblages) was studied with a conventional petrographic microscope, and microthermometric measurements were carried out with a USGS-style heating/freezing stage, which was calibrated using synthetic fluid inclusions, with precisions of ±0.3°C for measurements below 30°C and ±1.0°C for higher temperature runs. Gas composition of the fluid inclusions was analyzed by laser Raman microspectroscopy at CREGU-UMR G2R, Nancy, France, with a LABRAM Jobin-Yvon system. The exciting radiation is 514.5 nm, and the detection limits are about 1 mol% for CO_2 and N_2 and 0.1 mol% for CH_4 and H_2S. Opaque minerals in the inclusions were examined with a reflected light microscope, and selected samples were checked with Raman microspectroscopy. The concentrations of Cu in chalcopyrite-bearing fluid inclusions were calculated based on the volume ratios of chalcopyrite/fluid inclusion, the density of chalcopyrite (4.2 g/cm^3) and bulk inclusion fluid, and Cu content in chalcopyrite (34.6 wt%). The volume ratios of chalcopyrite/fluid inclusion were estimated from a modification of the area ratios, which were calculated with the AutoCAD program tracing the fluid and solid phases. Because the thicknesses of the fluid inclusions and opaque daughter minerals cannot be objectively measured, it is assumed that these objects are ellipsoidal and the third dimension is equal to the geometric mean of the two measured dimensions. Based on this assumption, the volume ratio=(area ratio)$^{3/2}$. The density and salinity of the fluid inclusions were calculated with the Flincor program of Brown (1989), with the fluid composition being approximated by H_2O–NaCl–CO_2. The calculated concentrations of Cu are of semiquantitative nature due to uncertainties of the volume ratios estimation.

Fluid inclusion occurrences and analytical results

The CO_2-bearing fluid inclusions occur in trails or clusters (Fig. 1b), or are relatively isolated, in stage I quartz of porphyry mineralization. They are rounded, irregular, or show negative crystal shape, and range in size from <1 to 16 μm. Halite-bearing aqueous inclusions occur relatively isolated (Fig. 1b), and aqueous inclusions without halite crystals (Fig. 1c) occur either in the same trails or clusters as the CO_2-bearing fluid inclusions (Fig. 1b) or in separate trails or clusters. In other samples from the Fenghuangshan deposit, halite-bearing aqueous fluid inclusions are the dominant type in stage I quartz, and aqueous inclusions without salt crystals are typical of stage III quartz (Lai et al., in preparation). The halite-bearing aqueous inclusions are interpreted as primary inclusions, whereas the CO_2-bearing fluid inclusions and the aqueous inclusions without halite crystals are considered as secondary ones in stage I quartz.

Most of the CO_2-bearing fluid inclusions consist of an aqueous phase plus one or two carbonic phases at room temperature (Fig. 1d–g), with variable carbonic/total area ratios ranging from 25 to 95%. Some CO_2-bearing fluid inclusions do not have a visible aqueous phase (Fig. 1h) and remained a single phase during the cooling runs. More than half of the CO_2-bearing fluid inclusions contain opaque minerals (Fig. 1d–h), which are less than 2 μm in size and show yellow reflectance (Fig. 1i,j). In contrast, few aqueous inclusions associated with the CO_2-bearing fluid inclusions contain opaque minerals.

The melting temperatures of the carbonic phase range from −59.2 to −56.2°C (Fig. 2a), indicating CO_2 as the dominant component. Raman analysis indicates the mole percentage of CO_2 in the carbonic phase from 90 to 100%, CH_4 from <0.5 to 1.5%, N_2 from <1 to 4%, H_2S from <0.5

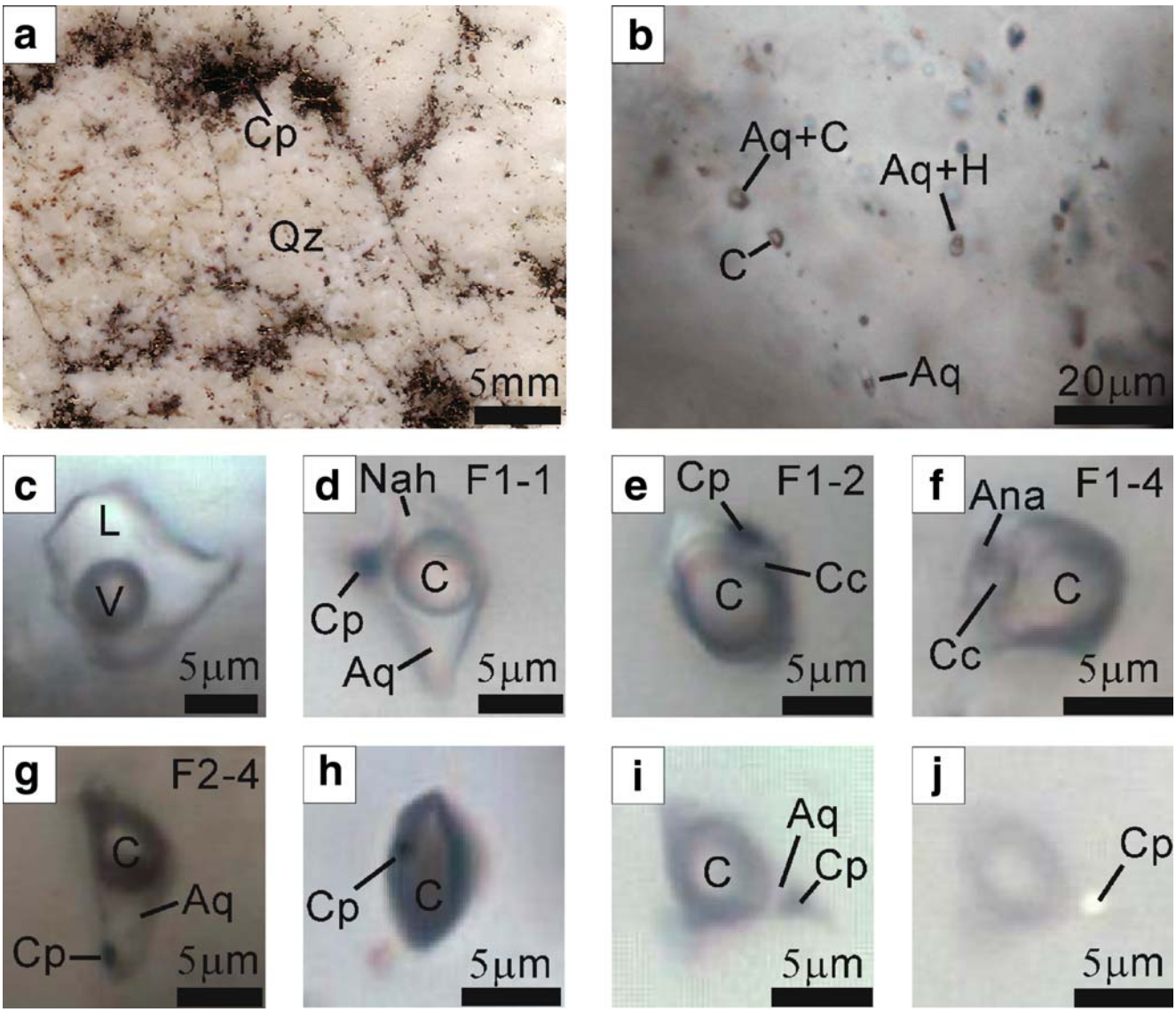

Fig. 1 **a** Chalcopyrite occurring as veinlets or patches in stage I quartz in quartz monzodiorite porphyry (scanned thin section). **b** Trails of CO_2-bearing fluid inclusions coexisting with aqueous inclusions in quartz secondary inclusions; note that a relatively isolated inclusion containing a halite daughter crystal (*Aq* + *H*, halite not visible on the photo) primary inclusions. **c** An aqueous inclusion without detectable CO_2. **d**–**g** CO_2 aqueous inclusions with different carbonic/total ratios and solid minerals of chalcopyrite, calcite, anatase, and nahcolite. Inclusion numbers marked at *top right corner* correspond to those in Table 1. **h** An carbonic inclusion (without a visible aqueous phase) containing a chalcopyrite crystal. **i** A CO_2 aqueous inclusion with a chalcopyrite crystal (plain polarized light). **j** Same as subpanel **i** but under cross polarized light; note the yellow reflectance of chalcopyrite. *Aq* Aqueous, *C* carbonic, *Cc* calcite, *Cp* chalcopyrite, *H* halite, *L* liquid, *Nah* nahcolite, *Qz* quartz, *V* vapor

to 8%, and C_2H_6 is detected (<0.1%) in one inclusion (Table 1). The homogenization temperatures of CO_2 range from 15.3–29.1 (to liquid) to 21.6–30.1°C (to vapor), and some inclusions show critical homogenization from 29.3 to 29.5°C (Fig. 2b). The temperatures of total homogenization of CO_2-bearing fluid inclusions range from 224 to 390°C (many were decrepitated between 260 and 400°C, before total homogenization), and those of aqueous inclusions are from 122 to 362°C (Fig. 2c). The clathrate-melting temperatures of the CO_2-bearing fluid inclusions range from −7.1 to +10.4°C, and the calculated salinities range from 0 to 21 wt% NaCl equivalent, mostly from 5 to 8.5 wt% (Table 2).

Raman spectra confirm that the opaque mineral with yellow reflectance color in CO_2-bearing fluid inclusions is chalcopyrite (Fig. 3a). In addition, nahcolite and calcite occur in some inclusions, and anatase is found in one inclusion (Figs. 1d–f and 3b–d). The volume percentage of the chalcopyrite ranges from 0.04 to 0.92% (Table 2). The calculated Cu concentrations range from 0.1 to 3.4 wt% (Table 2). The relationships between the calculated Cu concentrations and salinities, CO_2 mole fraction, and H_2S

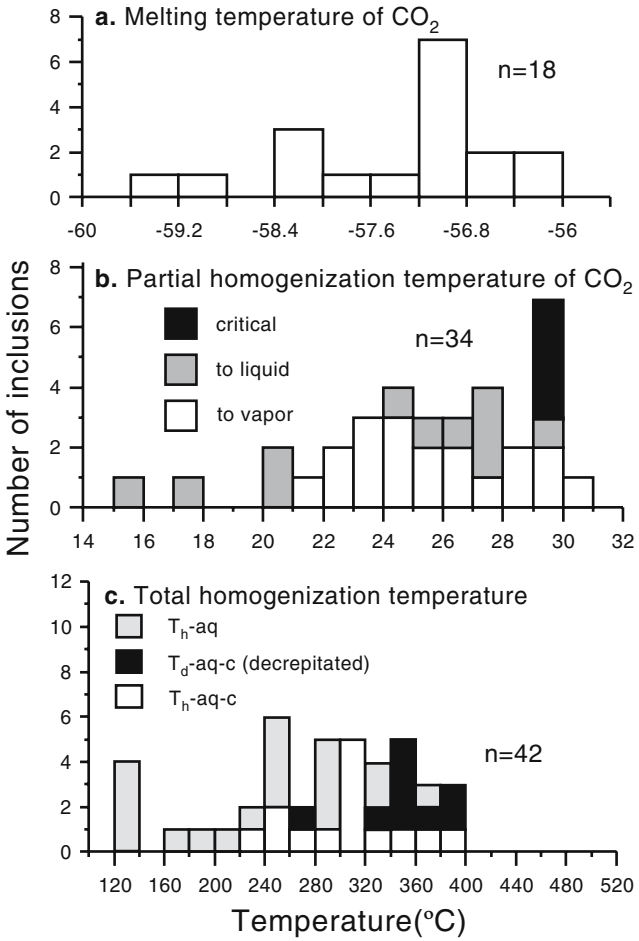

Fig. 2 Histograms of melting temperatures of CO_2 (**a**), homogenization temperatures of CO_2 phases (**b**), and total homogenization temperatures (**c**)

mole percentage in the carbonic phase are shown in Fig. 4. No apparent correlation is observed except the inclusion with the highest Cu concentration correspond to highest CO_2 mole fraction and H_2S mole percentage values.

Data interpretation and discussion

The spatial association of CO_2-bearing fluid inclusions with chalcopyrite suggests that the CO_2-bearing fluid was related to copper mineralization in the studied samples, although magmatic fluids with high salinities (represented by fluid inclusions with halite and sylvite daughter crystals) were mainly responsible for copper mineralization at the deposit scale (Lai et al., in preparation). However, it is not the purpose of this paper to discuss the importance of CO_2-bearing fluids for the formation of the Fenghuangshan deposit. We are concerned in this study with the capacity and form of CO_2-dominated fluid to transport copper, even though this may be of local significance for the deposit.

The chalcopyrite crystal in the CO_2-bearing fluid inclusions is interpreted to be a daughter mineral rather than solid inclusion entrapped by accident, considering its frequency of occurrence (in more than half of the CO_2-bearing fluid inclusions) and consistently small volume percentage (<1%). The calculated Cu concentrations (0.1 to 3.4 wt%) indicate that the fluid has the potential to transport large amounts of Cu.

The wide range of CO_2 contents of the fluid inclusions is interpreted to have resulted from heterogeneous trapping of two immiscible fluids, an aqueous fluid and a CO_2-dominated fluid. The coexistence of the two fluids is indicated by the occurrence of CO_2-rich and aqueous inclusions in the same healed fractures (Fig. 1b). Although we cannot rule out the possibility that the two fluids resulted from phase separation of an initially homogeneous fluid, we think they are more likely to be derived from two different sources because aqueous inclusions with characteristics similar to those in the samples of this study were widespread elsewhere in the Fenghuangshan deposit (without accompanying CO_2-bearing inclusions). The large variations of homogenization temperatures and salinities may reflect, in addition to heterogeneous trapping, the dynamic nature of the mineralizing environment, where

Table 1 Results of Raman spectroscopic analyses of the carbonic portion of CO_2-bearing fluid inclusions

Inclusion no.	Carbonic/total area ratio (%)	CO_2 (mol%)	CH_4 (mol%)	N_2 (mol%)	H_2S (mol%)	C_2H_6 (mol%)
F1-1	35	98.5	<0.5	≤1	nd	
F1-2	85	100	nd	nd	nd	
F1-4	85	93	1	≤1	5	
F2-1	35	94	1.5	≤1	4	
F2-2	80	94	1.3	≤1	4	
F2-3	95	95.5	<0.5	4	nd	
F2-4	45	92	2	≤1	5	<0.1
F2-5	85	98	<0.5	≤1	<0.5	
F2-6	65	99	<0.5	≤1	nd	
F2-7	85	90	2	≤1	8	
F2-8	90	98	<0.5	≤1	0.7	

Table 2 Calculated Cu concentrations (wt%) in CO_2-bearing fluid inclusions with chalcopyrite daughter mineral

No.	Raman sample no.	Area (μm^2)			Volume ratio (%)		T_m-cla (°C)	T_hc (°C)	Bulk density (g/cm^3)	Salinity (wt%) NaCl equivalent	X_{CO_2}	Cu (wt%)
		Total	CO_2	Cp	CO_2	Cp						
1	F1-1	61	20	1.6	19	0.42	7.4	24.2L	0.97	5.0	0.06	0.6
2	F1-2	46	29	1.3	50	0.47	7.0	27.7V	0.66	5.7	0.10	1.0
3	F2-1	66	47	0.3	59	0.04	6.6	29.4C	0.62	6.4	0.16	0.1
4	F2-2	39	28	0.4	60	0.12	5.5	27.0V	0.58	8.2	0.15	0.3
5	F2-4	40	18	0.8	30	0.28	7.4	29.5C	0.82	5.0	0.05	0.5
6	F2-6	26	12	1.1	32	0.83	5.3	27.5L	0.93	8.5	0.11	1.3
7	F2-7	41	35	1.8	81	0.92		25.0V	0.40		0.30	3.4
8		33	8	0.8	13	0.42	0.8	24.9V	0.99	14.6	0.02	0.6
9		14	5	0.4	24	0.44	3.3	25.4V	0.88	11.5	0.03	0.7
10		43	21	0.8	34	0.24	10.4	25.6L	0.89	0	0.13	0.4
11		52	28	0.8	39	0.17	7.1	26.9L	0.90	5.5	0.15	0.3
12		55	16	1.3	16	0.35	−7.1	29.1L	1.07	20.7	0.05	0.5
13		40	22	1.2	41	0.49	7.0	29.6V	0.75	5.7	0.09	1.0
14		21	7	0.6	19	0.49	−4.5	28.4V	0.98	19.4	0.03	0.7

Cp Chalcopyrite, T_m-*cla* clathrate melting temperature, *ThC* carbonic phase homogenization temperature

significant temperature and salinity change might have been caused by the interplay between hot magmatic fluids and relatively cool fluids from the country rocks. At the deposit scale, the mixing between a hot, saline, metal-carrying magmatic fluid and a relatively cool fluid from the country rocks was the main mechanism of ore precipitation (Lai et al., in preparation), while locally, a metal-carrying CO_2-dominated fluid was involved in the mineralization, as indicated by the chalcopyrite-bearing CO_2-dominated fluid inclusions.

It is not known how Cu was transported in the CO_2-dominated fluid, as there is no clear correlation between Cu and salinities (Fig. 4a) or H_2S (Fig. 4c). However, the fact that chalcopyrite daughter crystals are common in CO_2-bearing inclusions (including those lacking visible aqueous phase, thus low total salt contents) and rare in associated aqueous inclusions, and the presence of H_2S in most of the CO_2-bearing fluid inclusions suggest that H_2S may be responsible for Cu transport, perhaps in the form of HS^- complexes (Heinrich et al. 1999; Mountain and Seward 2003). The association between H_2S and CO_2 are likely related to their volatility, both being more volatile than H_2O and tending to be concentrated together in the vapor phase when a hydrothermal system undergoes phase separation

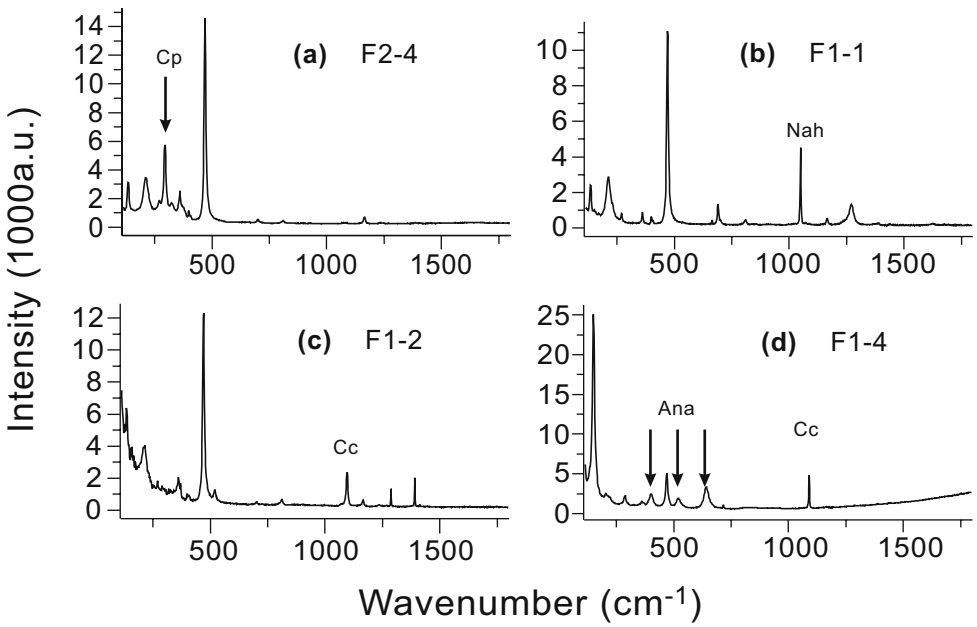

Fig. 3 Raman spectra of minerals within fluid inclusions: **a** chalcopyrite (*Cp*), **b** nahcolite (*Nah*), **c** calcite (*Cc*), and **d** calcite and anatase (*Ana*)

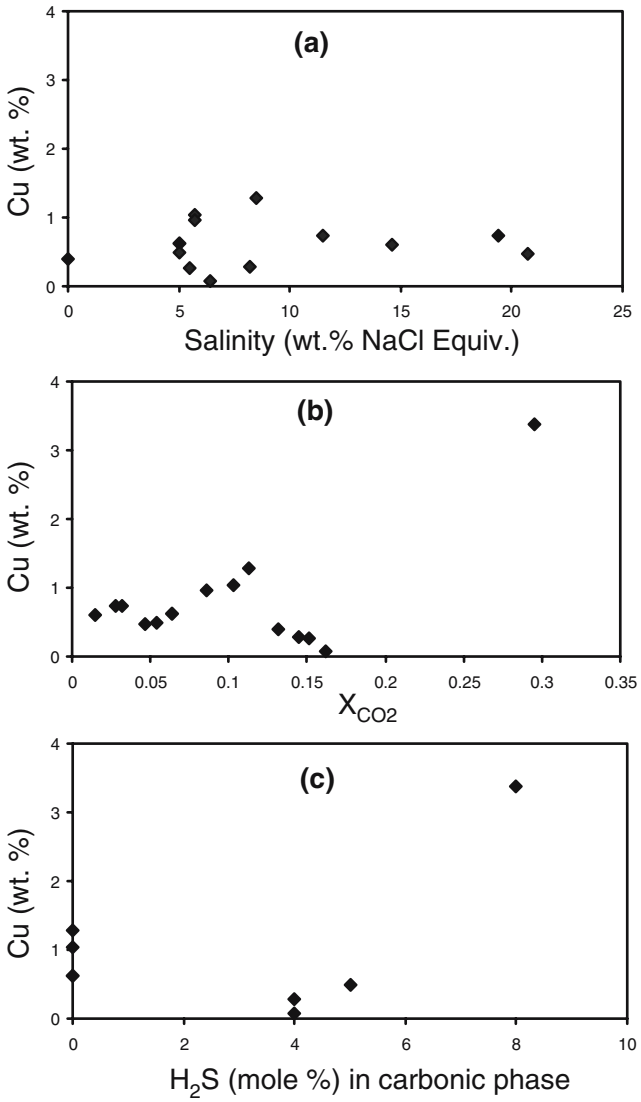

Fig. 4 Correlation diagrams between calculated Cu concentrations and salinity (**a**), CO_2 mole fraction (**b**), and H_2S mole percentage in the carbonic phase (**c**)

(Drummond and Ohmoto 1985). The CO_2- and H_2S-enriched vapor might have been derived from phase separation at a deeper site, or from accumulation of volatiles from various sources, including skarn formation processes.

CO_2 is generally not a major component in shallow magmatic systems because it preferentially escapes from the magma at relatively deep environments (Lowenstein 2001). This may explain why vapor inclusions in porphyry copper deposits, including those containing chalcopyrite daughter crystal (see Williams-Jones and Heinrich 2005), are not enriched in CO_2. It also indicates that CO_2, by itself, is not an important agent for Cu transport. However, in deeper mineralizing systems, such as orogenic gold deposits (Ridley and Diamond 2000) and granitic intrusion-related gold deposits (Baker 2002), CO_2 can be the major component. The affiliation between CO_2 and H_2S (due to their volatility), rather than CO_2 as a transporting agent, is likely responsible for the association of gold mineralization with CO_2-rich fluids. Furthermore, in contrast to the hypothesis that CO_2-enriched fluids resulted from in situ phase separation, it is likely that the CO_2-enriched fluids originated from different sources and were transporting gold to the sites of mineralization (Chi et al. 2005, 2006).

In conclusion, based on the observation of chalcopyrite daughter crystal in CO_2-bearing fluid inclusions from the Fenghuangshan Cu–Fe–Au deposit, we propose that CO_2-enriched fluids have the capacity to carry large amounts of copper. The CO_2-rich fluids are also enriched in H_2S, which is mainly responsible for Cu transport. By extension, the findings of this study suggest that in mineralizing systems where CO_2 is a major component, large amounts of metals might have been transported in vapor, which is channeled to the sites of mineralization.

Acknowledgements This study is supported by the tenth national "Five-year Project" of China (Project Nos. 2001BA609A-06 and 2004BA615A-02) and by the Chinese Scholarship Council (to Lai). Petrographic and microthermometric studies were carried out at the Geofluids Laboratory in the University of Regina with support from CFI and NSERC (to Chi). Laser Raman spectrum analyses were carried out by Therese Lhomme at CREGU-UMR G2R, Nancy, France. We would like to thank S. Peng, Y. Shao, B. Yang, Z. Cao, and S. Li for their help in the field work. Dr. Kalin Kouzmanov is thanked for his constructive review, which improved the quality of the paper.

References

Baker T (2002) Emplacement depth and carbon dioxide-rich fluid inclusions in intrusion-related gold deposits. Econ Geol 97:1111–1118

Barnes HL (1979) Solubility of ore minerals. In: Barnes HL (ed) Geochemistry of hydrothermal ore deposits. Wiley, pp 404–460

Brown PE (1989) FLINCOR: a microcomputer program for the reduction and investigation of fluid inclusion data. Am Mineral 74:1390–1393

Chang Y, Liu X, Wu Y (1991) The copper–iron belt of the lower and middle reaches of the Changjiang river. Geological Publishing House, Beijing, p 379 (in Chinese with English abstract)

Chi G, Williams-Jones AE, Dube B, Williamson K (2005) Carbonic vapor-dominated fluid systems in orogenic-type Au deposits. Geochim Cosmochim Acta 69:A738

Chi G, Dube B, Williamson K, Williams-Jones AE (2006) Formation of the Campbell–Red Lake gold deposit by H_2O-poor, CO_2-dominated fluids. Miner Depos 40:726–741

Drummond SE, Ohmoto H (1985) Chemical evolution and mineral deposition in boiling hydrothermal systems. Econ Geol 80:126–147

Hanley JJ, Mungall JE, Pettke T, Spooner ETC, Bray CJ (2005) Ore metal redistribution by hydrocarbon-brine and hydrocarbon-halide melt phases, North Range footwall of the Sudbury igneous complex, Ontario, Canada. Miner Depos 40:237–256

Heinrich CA, Günther D, Audétat A, Ulrich T, Frischknecht R (1999) Metal fractionation between magmatic brine and vapor, determined by microanalysis of fluid inclusions. Geology 27:755–758

Lowenstein JB (2001) Carbon dioxide in magmas and implications for hydrothermal systems. Miner Depos 36:490–502

Mountain BW, Seward TM (2003) Hydrosulfide/sulfide complexes of copper(I): experimental confirmation of the stoichiometry and stability of $Cu(HS)_2$ to elevated temperatures. Geochim Cosmochim Acta 67:3005–3014

Pan Y, Dong P (1999) The lower Changjiang (Yangzi/Yangtze River) metallogenic belt, Eastern Central China: intrusion- and wall rock-hosted Cu–Fe–Au, Mo, Zn, Pb, Ag deposits. Ore Geol Rev 15:177–242

Ridley JR, Diamond LW (2000) Fluid chemistry of orogenic lode gold deposits and implications for genetic models. In: Hagemann SG, Brown PE (eds) Gold in 2000. Rev Econ Geol 13:146–162

Schmidt Mumm A, Oberthür T, Vetter U, Blenkinsop TG (1997) High CO_2 content of fluid inclusions in gold mineralizations in the Ashanti Belt, Ghana: a new category of ore forming fluids? Miner Depos 32:107–118

Yang K, Scott SD (1996) Possible contribution of a metal-rich magmatic fluid to a sea-floor hydrothermal system. Nature 383:420–423

Williams-Jones AE, Heinrich CA (2005) Vapor transport of metals and the formation of magmatic-hydrothermal ore deposits. Econ Geol 100:1287–1312